J|A|C|S
ARTICLES
Published on Web 08/09/2002

The Electrophilic Reactions of Pentacyanonitrosylferrate(II) with Hydrazine and Substituted Derivatives. Catalytic Reduction of Nitrite and Theoretical Prediction of η^1-, η^2-N_2O Bound Intermediates

María M. Gutiérrez,[†] Valentín T. Amorebieta,*[,†] Guillermina L. Estiú,[‡,§] and José A. Olabe*[,§]

Contribution from the Department of Chemistry, Facultad de Ciencias Exactas, Universidad Nacional de Mar del Plata, Funes y Roca, Mar del Plata B7602AYL, Argentina, Cequinor, Department of Chemistry, Facultad de Ciencias Exactas, Universidad Nacional de La Plata, 47 y 115, La Plata, Argentina, and Department of Inorganic, Analytical, and Physical Chemistry, Inquimae, Facultad de Ciencias Exactas y Naturales, Universidad de Buenos Aires, Pabellón 2, Ciudad Universitaria, C1428EHA Buenos Aires, Argentina

Received February 21, 2002

Abstract: The electrophilic reactivity of the pentacyanonitrosylferrate(II) ion, $[Fe(CN)_5NO]^{2-}$, toward hydrazine (Hz) and substituted hydrazines (MeHz, 1,1-Me_2Hz, and 1,2-Me_2Hz) has been studied by means of stoichiometric and kinetic experiments (pH 6−10). The reaction of Hz led to N_2O and NH_3, with similar paths for MeHz and 1,1-Me_2Hz, which form the corresponding amines. A parallel path has been found for MeHz, leading to N_2O, N_2, and MeOH. The reaction of 1,2-Me_2Hz follows a different route, characterized by azomethane formation (MeNNMe), full reduction of nitrosyl to NH_3, and intermediate detection of $[Fe(CN)_5NO]^{3-}$. In the above reactions, $[Fe(CN)_5H_2O]^{3-}$ was always a product, allowing the system to proceed catalytically for nitrite reduction, an issue relevant in relation to the behavior of the nitrite and nitric oxide reductase enzymes. The mechanism comprises initial reversible adduct formation through the binding of the nucleophile to the N-atom of nitrosyl. The adducts decompose through OH^- attack giving the final products, without intermediate detection. Rate constants for the adduct-formation steps ($k = 0.43\ M^{-1}\ s^{-1}$, 25 °C for Hz) decrease with methylation by about an order of magnitude. Among the different systems studied, one-, two-, and multielectron reductions of bound NO^+ are analyzed comparatively, with consideration of the role of NO, HNO (nitroxyl), and hydroxylamine as bound intermediates. A DFT study (B3LYP) of the reaction profile allows one to characterize intermediates in the potential hypersurface. These are the initial adducts, as well as their decomposition products, the η^1- and η^2-linkage isomers of N_2O.

Introduction

The electrophilic reactions of the nitrosyl ligand in transition metal centers constitute one of its most important reactivity modes.[1] Particularly, the reactions of the pentacyanonitrosylferrate(II) ion, $[Fe(CN)_5NO]^{2-}$ (hereafter FeNO), with different nucleophiles have been known for many years.[2] Early use of these reactions as color tests for identifying SH^- or SO_3^{2-} [2,3] have been pursued by mechanistic studies in the 1970's.[4] The work has been extended to other MX_5 fragments, mainly with M = ruthenium and ancillary coligands as diverse as cyanides, amines, and polypyridines.[4,5] This reactivity mode is characteristic of the {MNO}[6] systems (Enemark−Feltham notation)[6] containing essentially linear MNO species, with values of ν_{NO}, the nitrosyl stretching wavenumber, greater than around 1860 cm^{-1}.[7]

The simplest example of the above reaction type comprises the reversible addition of the OH^- ion into the {MNO} moieties (the site of attack is the N-atom) forming $\{MNO_2H\}$ intermediates which further react with another OH^- to give the final $\{M-NO_2\}$ complexes.[1,4,5,8] Kinetic studies have been also performed with SH^-, SR^-, SO_3^{2-}, NH_3, and amines, N_3^-, NH_2OH, etc.[5] For these nucleophiles, the reversible adduct-formation reactions

* To whom correspondence should be addressed. V.T.A.: E-mail, amorebie@mdp.edu.ar. J.A.O.: E-mail, olabe@qi.fcen.uba.ar.
[†] Universidad Nacional de Mar del Plata.
[‡] Universidad Nacional de La Plata.
[§] Universidad de Buenos Aires.

(1) (a) Richter-Addo, G. B.; Legzdins, P. *Metal Nitrosyls*; Oxford University Press: NewYork, 1992. (b) Westcott, B. L.; Enemark, J. H. In *Inorganic Electronic Structure and Spectroscopy: Applications and Case Studies*; Solomon, E. I., Lever, A. B. P., Eds.; Wiley: New York, 1999; Vol. 2, pp 403−450. (c) Ford, P. C.; Lorkovic, I. M. *Chem. Rev.* **2002**, *102*, 993−1018.
(2) Swinehart, J. H. *Coord. Chem. Rev.* **1967**, *2*, 385−402.
(3) Boedeker, C. *Liebigs Ann. Chem.* **1861**, *117*, 193.
(4) McCleverty, J. A. *Chem. Rev.* **1979**, *79*, 53−76.
(5) Bottomley, F. In *Reactions of Coordinated Ligands*; Braterman, P. S., Ed.; Plenum: New York, 1985; Vol. 2, pp 115−222.
(6) Enemark, J. H.; Feltham, R. D. *Coord. Chem. Rev.* **1974**, *13*, 339−406.
(7) Bottomley, F. *Acc. Chem. Res.* **1978**, *11*, 158−163.
(8) (a) Swinehart, J. H.; Rock, P. A. *Inorg. Chem.* **1966**, *5*, 573−576. (b) Masek, J.; Wendt, H. *Inorg. Chim. Acta* **1969**, *3*, 455−458. (c) Chevalier, A. A.; Gentil, L. A.; Olabe, J. A. *J. Chem. Soc., Dalton Trans. (1972−1999)* **1991**, 1959−1963. (d) Baraldo, L. M.; Bessega, M. S.; Rigotti, G. E.; Olabe, J. A. *Inorg. Chem.* **1994**, *33*, 5890−5896.

are followed by irreversible processes affording the reduction of nitrosyl and oxidation of the nucleophiles. Questions still arise as to the nature and reactivity mode of the adduct intermediates, as well as on the identity of the precursors of gaseous products: N_2, N_2O, or mixtures of them.[5] Interest in the mechanisms of formation and release of these small molecules is alive, particularly for N_2O, whose coordination chemistry is poorly understood.[9] This type of redox reactivity is relevant for denitrification processes,[10] as well as for the uptake, transport, and delivery of NO in biological fluids, eventually mediated by iron enzymes.[11]

A communication has been published on the reaction of FeNO with hydrazine.[12] We found N_2O, NH_3, and $[Fe(CN)_5H_2O]^{3-}$ as products, in contrast with previous results involving related ruthenium and osmium nitrosyl complexes, which led to bound azide.[13] The reaction of FeNO with hydrazine is mechanistically interesting in its own right, because N_2O is an unusual product of hydrazine oxidations.[14] Besides, it shows that NO is avoided as an intermediate in the reduction process, on the basis of a two-electron transfer from hydrazine to the {FeNO} moiety showing no evidence for the intermediate stabilization of NO or "nitroxyl"-like species (HNO). The latter issues are of some controversy in the analysis of denitrification mechanisms involving nitrite and nitric oxide reductase enzymes.[10]

The formation of NO, N_2O, N_2, NH_2OH, or NH_3 as reduction products of {MNO} complexes depends on the reductant and on the metal-coligand environment.[15] The key initial step of nitrite coordination and proton-assisted dehydration forming a {MNO} moiety with some $\{M^{II}(NO^+)\}$ character is well understood, at least for the low-spin d^6 systems,[4,5,10,16] but this is not the case for the subsequent steps affording reduction. In our communication, we have advanced some results on the different pathways promoted by hydrazine and 1,2-dimethylhydrazine. The latter was found to react through the formation and decay of the $[Fe(CN)_5NO]^{3-}$ radical intermediate, and subsequent studies showed that NH_3 was the final six-electron reduction product of nitrosyl, instead of N_2O. We were prompted to perform a systematic investigation of the influence of substitution on hydrazine while keeping the electrophilic MNO moiety invariable. The pentacyanonitrosylferrate ion is a good candidate for studying alternative modes of adduct decompositions, according to the nucleophile, leading to different reduced nitrogen products, with the advantage that these reactions can operate in a catalytic way, as done by enzymes. These interesting complex reactions are also good targets for systematic theoretical explorations. Thus, we present a DFT analysis of complete reaction schemes for electrophilic reactions, which allow for the prediction and characterization of stable bound intermediates formed in the process of adduct formation and decomposition leading to N_2O release.

Experimental Section

General. Abbreviations. The following abbreviations are used: Hz, hydrazine; MeHz, methylhydrazine; 1,1-Me_2Hz, 1,1-dimethylhydrazine; 1,2-Me_2Hz, 1,2-dimethylhydrazine; $MeNH_2$, methylamine; Me_2NH, dimethylamine; MeNNMe, azomethane; MeOH, methanol.

Reagents. FeNO was from Merck. $Na_3[Fe(CN)_5NH_3]\cdot 3H_2O$ was synthesized starting from FeNO, according to literature procedures.[17] $Fe^{15}NO$ was prepared from $K_4[Fe(CN)_6]\cdot 3H_2O$ (Riedel-de-Haen) and $Na^{15}NO_2$ (Isotec, 99% ^{15}N).[18] ACS reagents $Hz\cdot SO_4H_2$ and 1,2-$Me_2Hz\cdot 2HCl$ (Aldrich) were used as received. MeHz (Aldrich) was purified by distillation in a nitrogen atmosphere. 1,1-$Me_2Hz\cdot HCl$ was synthesized by adaptation of Blatt's method.[19] Isonicotinamide and pyrazinamide were from Aldrich. Reagent grade NaCl, $Na_2B_4O_7\cdot 10H_2O$, H_2KPO_4 (Merck), and NaOH (Anwill) were used for buffer and ionic strength adjustments. A Hanna pH meter, model HI9321, was calibrated against standard buffers (Merck). Deionized distilled water was used in all of the experiments.

Stoichiometric and Kinetic Measurements. The $[Fe(CN)_5H_2O]^{3-}$ complex formed in all of the studied reactions is a well-characterized ion (λ_{max}, 440 nm; ϵ, 640 M^{-1} cm^{-1}).[20] It reacts rapidly forming stable complexes with many ligands (with k_f = ca. 40−400 M^{-1} s^{-1} and K_{st} = ca. 10^4−10^5 M^{-1}).[21,22] Thus, in our reaction conditions containing an excess of hydrazine species, the aqua-ion can be determined through the formation of the corresponding $[Fe(CN)_5(hydrazine)]^{3-}$ complexes, with maxima at 400 nm.[21] A greater sensitivity for the quantification of $[Fe(CN)_5H_2O]^{3-}$ is obtained by adding *N*-heterocyclic derivatives as scavengers for the aqua-ion, thus getting more intensively colored complexes, $[Fe(CN)_5L]^{3-}$.[21,22] We used L = isonicotinamide (λ_{max} 440 nm; ϵ_{max} 4570 M^{-1} cm^{-1})[22] or pyrazinamide (λ_{max} 495 nm; ϵ_{max} 4750 M^{-1} cm^{-1}), depending on the system.

The other products $MeNH_2$, Me_2NH, MeNNMe, NH_3, N_2O, and N_2 (including labeled species) were identified by mass spectrometry, in a quadrupolar equipment Extrel, model Emba II. Mass balances for the total reactive nitrogen were performed for each of the reactions with different hydrazines. The residual quantities of Hz and Me_2Hz were determined by redox titrations.[23a] NH_3 was extracted from the residual solutions by distillation under N_2 flow and was quantified by acid/base titration. Alternatively, it was quantified spectrophotometrically on the residual solutions by means of its reaction product with phenol, NaClO, and nitroprusside as catalyst.[24] Me_2NH was quantified on the residual solution by specific acid/base titration.[23b] MeOH was extracted from the residual solutions by distillation; it was characterized and quantified as H_2CO, with chromotropic acid (UCB).[25]

(9) Trogler, W. C. *Coord. Chem. Rev.* **1999**, *187*, 303−327.
(10) (a) Averill, B. A. *Chem. Rev.* **1996**, *96*, 2951−2964. (b) Hollocher, T. C. In *Nitric Oxide Principles and Actions*; Lancaster, J., Jr., Ed.; Academic Press: New York, 1996.
(11) (a) Clarke, M. J.; Gaul, J. B. *Struct. Bonding (Berlin)* **1993**, *81*, 147−181. (b) *Nitric Oxide, Biology, and Pathobiology*; Ignarro, L. J., Ed.; Academic Press: New York, 2000.
(12) Chevalier, A. A.; Gentil, L. A.; Amorebieta, V. T.; Gutiérrez, M. M.; Olabe, J. A. *J. Am. Chem. Soc.* **2000**, *122*, 11238−11239.
(13) (a) Bottomley, F.; Crawford, J. R. *J. Am. Chem. Soc.* **1972**, *94*, 9092−9095. (b) Douglas, P. G.; Feltham, R. D.; Metzger, H. G. *J. Am. Chem. Soc.* **1971**, *93*, 84−90. (c) Bottomley, F.; Kiremire, E. M. R. *J. Chem. Soc., Dalton Trans. (1972−1999)* **1977**, 1125−1131.
(14) Stanbury, D. M. *Prog. Inorg. Chem.* **1998**, *47*, 511−561.
(15) (a) Armor, J. *Inorg. Chem.* **1973**, *12*, 1959−1961. (b) Armor, J. N.; Hoffman, M. Z. *Inorg. Chem.* **1975**, *14*, 444−446.
(16) (a) Barley, M. H.; Takeuchi, K. J.; Meyer, T. J. *J. Am. Chem. Soc.* **1986**, *108*, 5876−5885. (b) Murphy, W. R.; Takeuchi, K.; Barley, M. H.; Meyer, T. J. *Inorg. Chem.* **1986**, *25*, 1041−1053.
(17) Kenney, D. J.; Flynn, T. P.; Gallini, J. B. *J. Inorg. Nucl. Chem.* **1961**, *20*, 75.
(18) (a) van Voorst, J. D. W.; Hemmerich, P. *J. Chem. Phys.* **1966**, *45*, 3914−3918. (b) Wanner, M.; Scheiring, T.; Kaim, W.; Slep, L. D.; Baraldo, L. M.; Olabe, J. A.; Zalis, S.; Baerends, E. J. *Inorg. Chem.* **2001**, *40*, 5704−5707.
(19) Blatt, A. H., Ed. *Organic Synthesis*; Wiley: New York, 1943; Vol. 2.
(20) Toma, H. E. *Inorg. Chim. Acta* **1975**, *15*, 205−211.
(21) (a) Katz, N. E.; Olabe, J. A.; Aymonino, P. J. *J. Inorg. Nucl. Chem.* **1977**, *39*, 908−910. (b) Macartney, D. H. *Rev. Inorg. Chem.* **1988**, *9*, 101−151. "d−d" transitions around 400 nm (ϵ, 500−600 M^{-1} cm^{-1}) are characteristic of small nitrogenated molecules (NH_3, H_2H_4, NH_2OH) binding to $[Fe(CN)_5(H_2O)]^{3-}$ through σ-bonds. This is in contrast with more intense MLCT bands arising from the coordination of pyridine- and pyrazine-derivatives ($\epsilon = 4-8 \times 10^3$ M^{-1} cm^{-1}).[22]
(22) (a) Toma, H. E.; Malin, J. M. *Inorg. Chem.* **1973**, *12*, 1039−1044. (b) Toma, H. E.; Malin, J. M. *Inorg. Chem.* **1973**, *12*, 2080−2083. (c) Toma, H. E.; Malin, J. M. *Inorg. Chem.* **1974**, *13*, 1772−1774.
(23) (a) Siggia, S.; Hanna, J. G. *Quantitative Organic Analysis via Functional Groups*, 4th ed.; Wiley: New York, 1979; p 668. (b) Siggia, S.; Hanna, J. G. *Quantitative Organic Analysis via Functional Groups*, 4th ed.; Wiley: New York, 1979; p 581.
(24) Koroleff, F. In *Methods of Seawater Analysis*; Grasshoft, K., Ed.; Verlag Chemie: New York, 1976; pp 126−133.
(25) West, P. W.; Sen, B. *J. Anal. Chem.* **1956**, *153*, 12−18.

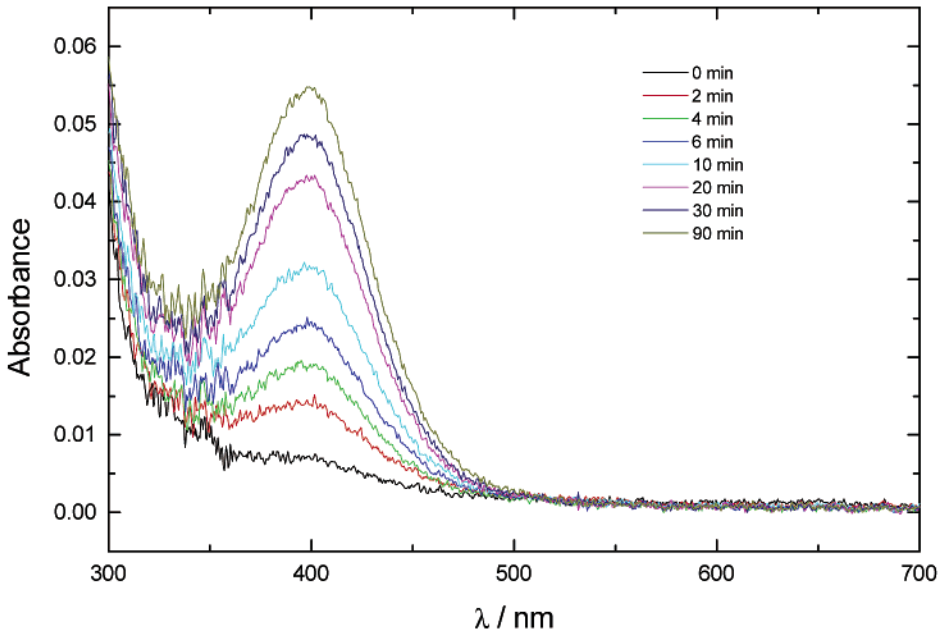

Figure 1. Successive UV−vis spectra for the reaction of $[Fe(CN)_5NO]^{2-}$ (1×10^{-4} M) with Hz (4.5×10^{-3} M), pH 9.4, $T = 25.0$ °C, $I = 0.1$ M. No scavenger added.

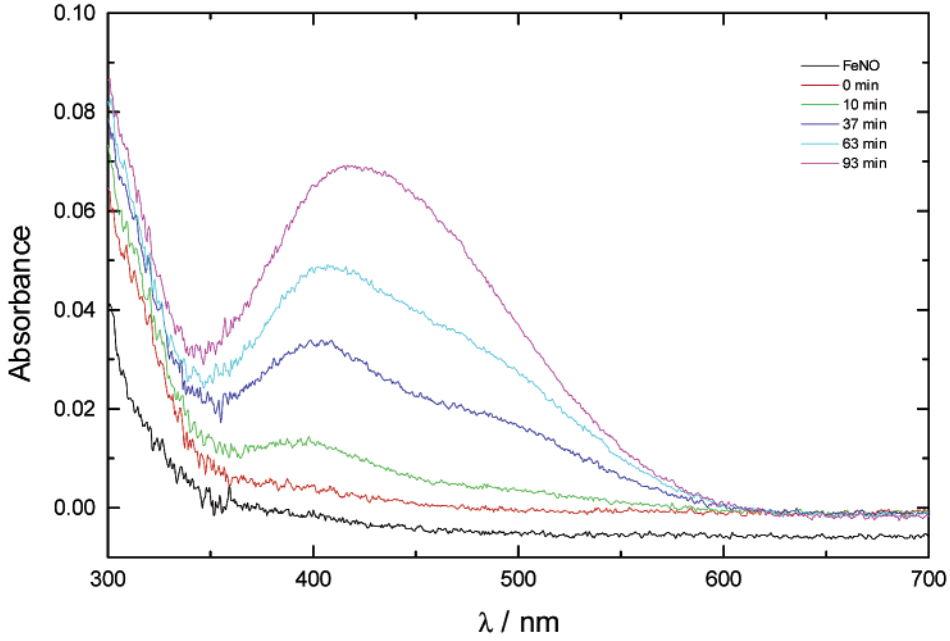

Figure 2. Successive UV−vis spectra for the reaction of $[Fe(CN)_5NO]^{2-}$ (1×10^{-4} M) with MeHz (2.8×10^{-3} M), pH 9.4, $T = 25.0$ °C, $I = 0.1$ M. No scavenger added.

The gas production measurements were carried out using a thermostatized homemade flow reactor (volume, 0.07 dm^3) supplied with an absolute pressure transducer MKS Baratron model 622 A and a mechanical stirrer. The reactor was linked to a vacuum system and to the mass spectrometer through a thin thermostatized capillary.

The kinetic studies were mainly performed by UV−vis spectrophotometry, in a Shimadzu UV 2101-PC instrument, under N_2 atmosphere and careful previous degassing, by measuring the absorbance increase of the $[Fe(CN)_5L]^{n-}$ product (L = scavenger *N*-heterocyclic ligand, see above). A blank experiment was done with FeNO and L in the absence of nucleophile, showing no reaction. To discard possible medium effects upon addition of L, direct measurements were made in its absence, by following the absorbance increase of the $[Fe(CN)_5N_2H_4]^{3-}$ ion, without significant differences in the rates. With Hz and Me_2Hz as nucleophiles, the rates were also obtained by measuring the amount of gas evolution as a function of time (these experiments were made without scavenger); they were found to be fairly similar (slower by a factor of 2) to those measured by spectrophotometric techniques. For 1,2-Me_2Hz, complementary kinetic measurements were done by following the absorption of the $[Fe(CN)_5NO]^{3-}$ intermediate (λ_{max} 345 and 440 nm, ϵ 3500 and 550 M^{-1} cm^{-1}, respectively),[26] pH 9.4, with no added scavenger. The onset and decay of the above radical species were also confirmed by EPR measurements, using a Bruker ER 200D X-band spectrometer. The concentration of FeNO was varied in the range 0.1−1 mM, under pseudo-first-order conditions with respect to the hydrazines (at least a factor of 10 was used). The pH range was 6−10.5, and constant temperature, 25.0 ± 0.5 °C, was generally used,

(26) Cheney, R. P.; Simic, M. G.; Hoffman, M. Z.; Taub, I. A.; Asmus, K. D. *Inorg. Chem.* **1977**, *16*, 2187−2192.

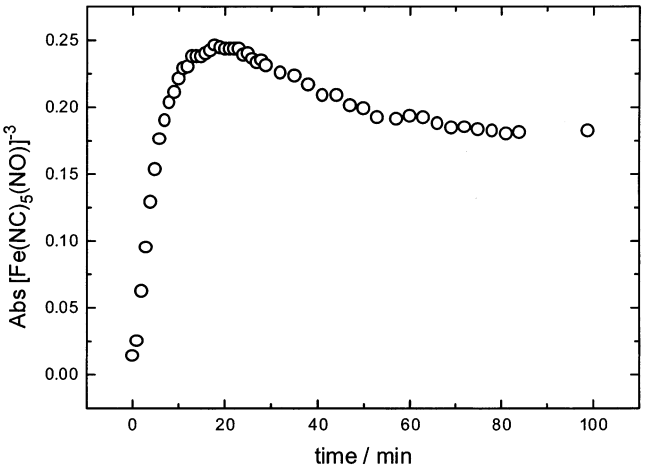

Figure 3. Time evolution of the absorbance of $[Fe(CN)_5NO]^{3-}$ in the reaction of $[Fe(CN)_5NO]^{2-}$ (2.8×10^{-4} M) with 1,2-Me_2Hz (2.6×10^{-3} M), measured at 340 nm, pH 9.4, $T = 47$ °C. No scavenger added.

except in the studies with 1,2-Me_2Hz, which were also performed at 47.0 °C, and with Hz, range 20.0−50.0 °C. Ionic strength was adjusted to $I = 0.1$ M (NaCl). The consumption of OH^- in the addition reactions was quantified through pH-stat titrations (Metrohm).

A typical stoichiometric and kinetic assay was done as follows: fresh concentrated solutions of each reactant (FeNO and nucleophile) were diluted with 3 mL of buffer ($c > 10^{-2}$ M, eventually with 0.1 M L scavenger, $I = 0.1$ M, NaCl) in the spectrophotometric cell. The solutions were previously degassed with UAP N_2 flow before mixing. The concentrations of reactants (FeNO, ca. 10^{-4} M; nucleophile, ca. 10^{-3} M) were calculated by dilution and are accurate within 5%. At the end of the reaction, the concentration of $[Fe(CN)_5L]^{3-}$ (L = scavenger) was determined and compared with the initial FeNO. These measurements were done around 1−12 h following the mixing of reactants, depending on the nucleophile.

For assessing the yield of other products, concentrations of reactants at least 10-fold greater than before were employed. First, 25−40 mL of a hydrazine solution containing the buffer and the solid FeNO were placed separately inside the reactor (see before). The reactants were mixed after evacuation of the system. The composition and quantitative evolution of the gaseous stream were monitored in real time. At the end of gas generation, the number of moles was determined and compared with the initial moles of FeNO. After elimination of the gaseous products, an aliquot of the solution was gasified for the mass spectral analysis of the remaining products. To minimize the superposition of the spectra between reactants and products, these essays were conducted with defect of nucleophile. Once identified, an adequate technique was selected for the separation and further quantification of the target (see before). For example, residual hydrazine present after the end of the reaction was determined directly in the final solutions by iodometry. For the determination of NH_3, the residual solutions were treated with iodine to eliminate excess hydrazine and were further titrated with phenol (see above). To establish both yields, at least two equivalent experiments were performed, one for NH_3 and the other for the remanent hydrazine.

For the treatment of kinetic data, the absorbance values were fitted to $\ln[(A_{oo} - A_t)/(A_{oo} - A_o)]$ versus time. A_{oo} and A_o were the absorbances at the completion and beginning of reaction, respectively, and A_t was the measured value at time t. A values were obtained at the appropriate wavelength for product formation (most times $[Fe(CN)_5L]^{3-}$ or eventually $[Fe(CN)_5(hydrazine)]^{3-}$). The pseudo-first-order rate constants (k_{obs}, s^{-1}) were plotted against the concentration of nucleophile, thus getting the specific second-order rate constants, k_{exp} (M^{-1} s^{-1}), at a given pH. Eyring plots were used for obtaining the activation parameters for the reaction of FeNO with Hz, by using k_{exp} values measured in the pH-independent region (Figure 4).

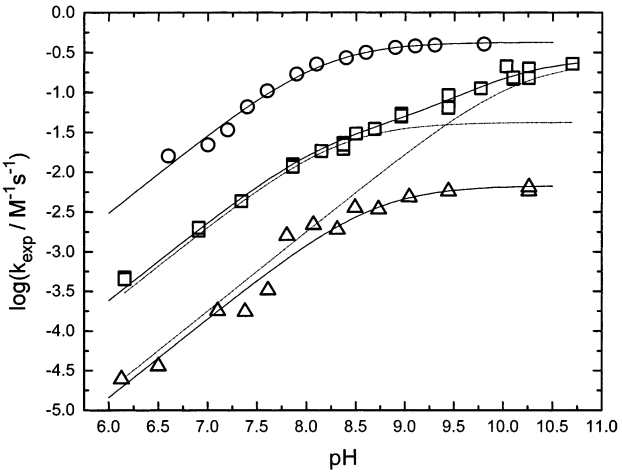

Figure 4. Dependence of log k_{exp} with pH in the reaction of $[Fe(CN)_5NO]^{2-}$ with hydrazines. Upper curve, Hz; intermediate curve, MeHz; lower curve, 1,1-Me_2Hz. $T = 25.0$ °C, $I = 0.1$ M. For MeHz, the broken lines represent the individual contributions of each term in eq 10.

Computational Details. Calculations have been performed using Gaussian 98[27] and Becke's three-parameter hybrid functional[28] with LYP correlation functional (B3LYP).[29] The basis was of double-ζ split valence plus polarization quality (6-31G(d,p)). The structures have been fully optimized with no symmetry constraints. The true nature of the optimized minima has been verified, in each case, by means of frequency calculations. Time-dependent DFT (TD-DFT) calculations[30,31] were conducted to study the singlet excited states of the complexes. Transition states have been optimized, at the same level, following a quadratic synchronous transit algorithm. They were fully characterized by means of a vibrational analysis, leading to one imaginary frequency.

Results

A. Stoichiometric Studies. A1. Reaction of FeNO with Hz. The stoichiometry can be described by eq 1. Figure 1 displays the spectra measured at different times at pH 9.4, *with no added scavenger*. Equation 1 is *rapidly* followed by eq 1′ (see Experimental Section).

$$[Fe(CN)_5{}^{15}NO]^{2-} + H_2NNH_2 + OH^- \rightarrow [Fe(CN)_5H_2O]^{3-} + NH_3 + N^{15}NO \quad (1)$$

$$[Fe(CN)_5H_2O]^{3-} + L \rightarrow [Fe(CN)_5L]^{3-} + H_2O \quad (L = N\text{-heterocyclic scavenger, or Hz}) \quad (1')$$

The conversion of FeNO into $[Fe(CN)_5L]^{3-}$ is essentially quantitative. Independent measurements of the number of moles of products, N_2O and NH_3, indicate a 1:1 ratio, with a yield

(27) Frisch, M. J.; Trucks, G. W.; Schlegel, H. B.; Scuseria, G. E.; Robb, M. A.; Cheeseman, J. R.; Zakrzewski, V. G.; Montgomery, J. A.; Stratman, R. E.; Burant, J. C.; Dapprich, S.; Millam, J. M.; Daniels, A. D.; Kudin, K. N.; Strain, M. C.; Farkas, O.; Tomasi, J.; Barone, V.; Cossi, M.; Cammi, R.; Mennucci, B.; Pomelli, C.; Adamo, C.; Clifford, S.; Ochterski, J.; Petersson, G. A.; Ayala, P. Y.; Cui, Q.; Morokuma, K.; Malick, D. K.; Rabuck, A. D.; Raghavachari, K.; Foresman, J. B.; Cioslowski, J.; Ortiz, J. V.; Baboul, A. G.; Stefanov, B. B.; Liu, C.; Liashenko, A.; Piskorz, P.; Komaromi, I.; Gomperts, R.; Martin, R. L.; Fox, D. J.; Keith, T.; Al-Laham, M. A.; Peng, C. Y.; Nanayakkara, A.; Gonzalez, C.; Challacombe, M.; Gill, P. M. W.; Johnson, B. G.; Chen, W.; Wong, M. W.; Andres, J. L.; Gonzales, C.; Head-Gordon, M.; Replogle, E. S.; Pople, J. A. *Gaussian 98*; Gaussian, Inc.: Pittsburgh, PA, 1998.
(28) Becke, A. D. *J. Chem. Phys.* **1993**, *98*, 5648−5652.
(29) Lee, C.; Yang, W.; Parr, R. G. *Phys. Rev.* **1988**, *B37*, 785−789.
(30) Casida, M. E.; Jamorski, C.; Casida, K. C.; Salahub, D. R. *J. Chem. Phys.* **1998**, *108*, 4439−4449.
(31) Stratmann, R. E.; Scuseria, G. E.; Frisch, M. J. *J. Chem. Phys.* **1998**, *109*, 8218−8224.

higher than 95% with respect to the initial FeNO. By working with $Fe^{15}NO$, the mass profile shows unequivocally that the label appears quantitatively as $^{14}N^{15}NO$,[32] but not as $^{15}NH_3$. Equation 1 is supported by complementary determinations of Hz and OH^- consumption. Equation 1′ is a common feature of all of the studied reactions and will be omitted further on.

A2. Reaction of FeNO with MeHz. Figure 2 shows the successive spectra at pH 9.4, *with no scavenger added*. At pH lower than 7, the products are $[Fe(CN)_5H_2O]^{3-}$, $MeNH_2$, and $N^{15}NO$. The stoichiometry is described in eq 2, which is similar to eq 1.

$$[Fe(CN)_5{}^{15}NO]^{2-} + MeHNNH_2 + OH^- \rightarrow [Fe(CN)_5H_2O]^{3-} + MeNH_2 + N^{15}NO \quad (2)$$

The mass balance shows that 1 mol of N_2O is formed per mole of initial FeNO. No ^{15}N label appears in $MeNH_2$.

At pH's higher than 8, the distribution of products is different. In addition to the products of eq 2, N_2 and MeOH are also produced. The mass balance accounts for 0.7 mol of N_2O and 0.3 mol of N_2 and MeOH, per mole of initial FeNO. This supports the simultaneous occurrence of eqs 2 and 3:

$$2[Fe(CN)_5{}^{15}NO]^{2-} + MeHNNH_2 + 2OH^- \rightarrow 2[Fe(CN)_5H_2O]^{3-} + N^{15}N + N^{15}NO + MeOH \quad (3)$$

The experiments at pH 9.4 show that the only *initial* gaseous product is N_2O. However, the relative yield of N_2 versus N_2O increases with the progress of reaction. The molar fraction of N_2O decreases from a value close to 1 down to 0.7. The labeling experiment with initial $Fe^{15}NO$ shows that ^{15}N is distributed among $N^{15}N$ and $N^{15}NO$,[32] of molar masses 29 and 45, respectively. Figure 2 shows that, in addition to the characteristic maximum of $[Fe(CN)_5MeHz]^{3-}$ at 400 nm, a shoulder develops at ca. 480 nm, suggesting a mixture of complexes.[33] The intensity of the shoulder increases with the progress of the reaction, with no further decay after 80−90% of initial FeNO is transformed into $[Fe(CN)_5MeHz]^{3-}$.[33]

A3. Reaction of FeNO with 1,1-Me_2Hz. The reaction products are $[Fe(CN)_5H_2O]^{3-}$, Me_2NH, and $N^{15}NO$. No ^{15}N label appears in Me_2NH. We propose eq 4 to support a common pattern with eqs 1 and 2.

$$[Fe(CN)_5{}^{15}NO]^{2-} + Me_2NNH_2 + OH^- \rightarrow [Fe(CN)_5H_2O]^{3-} + Me_2NH + N^{15}NO \quad (4)$$

When the reaction is performed without scavenger, the spectrum of the final solution is centered at 400 nm (corresponding to $[Fe(CN)_5(1,1\text{-}Me_2Hz)]^{3-}$), with a very weak shoulder at 480 nm (see SI Figure 1). As previously commented,[33] we estimate that the highest concentration of the species absorbing at 480 nm is close to 10^{-4} M, that is, 10% of initial FeNO. The FeNO consumption, as measured by the moles of the $[Fe(CN)_5(isonicotinamide)]^{3-}$ complex produced, was superior to 90%. Independent measurements of the number of moles of products, N_2O and Me_2NH, indicate a 1:1 ratio, with a yield of 80−90% with respect to the initial FeNO. Complementary determinations of 1,1-Me_2Hz consumption support eq 4 for the stoichiometry of the main reaction path.

A4. Reaction of FeNO with 1,2-Me_2Hz. A new picture appears with this reaction. The successive spectra with no scavenger added (not shown) are dominated by the development of a band centered at 340 nm (ϵ = ca. 3500 M^{-1} cm^{-1}), with a broad absorption at ca. 437 nm (ϵ = ca. 550 M^{-1} cm^{-1}). EPR measurements show that the well-characterized $[Fe(CN)_5NO]^{3-}$ intermediate[18] is rapidly formed (see SI Figure 2). The band pattern is likely due to a mixture of $[Fe(CN)_5NO]^{3-}$, $[Fe(CN)_5(1,2\text{-}Me_2Hz)]^{3-}$, and $[Fe(CN)_5NH_3]^{3-}$. The reaction at 25 °C is very slow, as compared with those corresponding to Hz and MeHz. Figure 3 displays the absorbance changes at 340 nm, 47 °C, showing an increase of $[Fe(CN)_5NO]^{3-}$,[26] which confirms its fast formation, with further slow decay. After 3−4 h, the identified reaction products are $[Fe(CN)_5H_2O]^{3-}$, $^{15}NH_3$, and MeNNMe. The residual absorption band is clearly centered at 400 nm, with ϵ = 600 M^{-1} cm^{-1}. All of the initial ^{15}N appears as $^{15}NH_3$, with no label at MeNNMe. The stoichiometric ratio of FeNO versus 1,2-Me_2Hz is 0.33. Overall, these results support eq 5 as describing the main reaction stoichiometry:

$$[Fe(CN)_5{}^{15}NO]^{2-} + 3MeHNNHMe + OH^- \rightarrow [Fe(CN)_5H_2O]^{3-} + {}^{15}NH_3 + 3MeNNMe + H_2O \quad (5)$$

The yield of NH_3 based on consumed FeNO and 1,2-Me_2Hz is close to 80−90%. The decay of $[Fe(CN)_5NO]^{3-}$ has not been studied in detail, but the final absorption at 400 nm, associated with the conversion of $[Fe(CN)_5H_2O]^{3-}$ to $[Fe(CN)_5(1,2\text{-}Me_2Hz)]^{3-}$, as well as the reaction of the residual solution with pyrazinamide, offer strong evidence of nearly complete aquation (80−90%) of any pentacyano-X-ferrate complexes. Complementary kinetic experiments describing the rate of formation of the $[Fe(CN)_5H_2O]^{3-}$ ion are presented in the following section.

B. Kinetic Studies. The kinetic experiments show a pseudo-first-order behavior up to nearly three half-lives for Hz, MeHz, and 1,1-Me_2Hz. At constant pH, the plots of the rate constants (k_{obs}, s^{-1}) against the concentration of the nucleophiles are linear, allowing for the calculation of the second-order rate constants (k_{exp}, M^{-1} s^{-1}) (Figures SI 3a,b, 4a,b, 5a,b). Activation parameters for the reaction with Hz are $\Delta H^{\ddagger} = 26.8 \pm 0.2$ kJ mol^{-1} and $\Delta S^{\ddagger} = -163 \pm 5$ J K^{-1} mol^{-1} (Figure SI 6). Figure 4 shows the variation of k_{exp} against pH. The apparent order of the reaction with respect to $[OH^-]$ is 1 in the limit of low pH and 0 at high pH. This behavior becomes especially evident for Hz and 1,1-Me_2Hz and is consistent with $k_{exp} = k/(1 + 10^{(pK - pH)})$. In this two-parameter equation, k depends on the reaction set, and pK can be reasonably related, in principle, to the protonation equilibria of hydrazine-species. The nonlinear fit of the data of Figure 4 to the above equation yields pK values

(32) The central ^{15}N label is demonstrated by the analysis of the fragmentation spectrum of N_2O. The molecular ion NNO^+ (relative yield 100) decays unimolecularly either through NN cleavage, generating the NO^+ ion (relative yield 30%), or through cleavage of the NO bond, generating the NN^+ ion (relative yield 10%). The position of the label is determined by the mass/charge relation of NO^+ (as the ions are of charge +1, the molar mass of the relevant ions is derived). For all of the experiments with $Fe^{15}NO$ and the hydrazines, we observed that the molecular ions coming from the N_2O products had a molar mass 45 (i.e., with only one ^{15}N-atom) and that the NO^+ ions always had a molar mass 31, revealing that a central ^{15}N-atom was present.

(33) While the main absorption at 400 nm is clearly assigned to $[Fe(CN)_5(MeHz)]^{3-}$, the shoulder must correspond to an intermediate with an intense absorption (see text). Considering $A_{480} = 0.025$, and assuming $\epsilon = 1000$ M^{-1} cm^{-1} as a lower limit, we estimate a concentration of ca. 2.5×10^{-5} M for the species remanent after the last spectrum in Figure 2. This represents around 25% of initial FeNO, as a maximum limit.

Table 1. Kinetic Parameters for Adduct Formation and Decomposition in the Reactions of $[Fe(CN)_5NO]^{2-}$ with Hydrazine and Substituted Derivatives[a]

	NH_2NH_2	NH_2NHCH_3	$NH_2N(CH_3)_2$	$CH_3NHNHCH_3$
pK_a[b]	7.97[c], 8.07[d]	7.87[d]	7.21[d]	~7.7[e]
$k_{6a}/M^{-1}\,s^{-1}$	0.43	0.044	6.2×10^{-3}	
pK	8.14	8.3	8.5	
$k_7/k_{-6a}/M^{-1}$	7.2×10^5	5.0×10^5	3.2×10^5	
$k_{6b}/M^{-1}\,s^{-1}$		0.21		0.03[f]
$(k_8/k_{-6b})/M^{-1}$		1.5×10^4		4.0×10^4 [f]

[a] $T = 25.0$ °C. See text for the underlying mechanism. [b] Corresponds to the monoprotonated species. [c] Reference 14. [d] Reference 37b. [e] Dennis, C. R.; Van Wyk, A. J.; Leipoldt, J. G. *Inorg. Chem.* **1987**, *26*, 270. [f] The kinetic rate constants were obtained as fitting parameters of the experimental absorption versus time values for $[Fe(CN)_5(pyrazinamide)]^{3-}$ and for $[Fe(CN)_5NO]^{3-}$, at 25 °C, to the model described by eqs 11−17, employing a standard computer program for chemistry simulation.

of 8.3 and 8.5 for Hz and 1,1-Me_2Hz, respectively. Their comparison with the pK_a values for the free hydrazinium species (cf. Table 1) shows that the agreement is good only for Hz. The disagreement between the observed curvature and pK_a for 1,1-Me_2Hz precludes this effect of being a substrate titration. Therefore, the observed pH-dependence may be ascribed to a genuine kinetic effect. For MeHz, k_{exp} represents the combined reactivity of both asymmetric N-atoms, and the curve region is not clearly visualized.

For the reaction of FeNO with 1,2-Me_2Hz, Figure 5 shows the absorbance *rate* against time, a variable that is proportional to the rate of production of $[Fe(CN)_5H_2O]^{3-}$ (calculated numerically from the pertinent absorbance vs time curve). The comparison with Figure 3 shows a clear displacement of the maxima. This fact reveals that the $[Fe(CN)_5NO]^{3-}$ ion cannot be the unique source of $[Fe(CN)_5H_2O]^{3-}$.

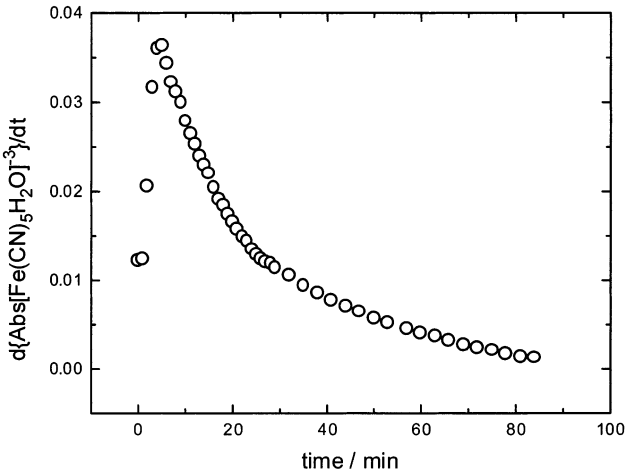

Figure 5. Time evolution of the derivative of the absorbance of $[Fe(CN)_5L]^{3-}$ (L = pyrazinamide) in the reaction of $[Fe(CN)_5NO]^{2-}$ (2.8×10^{-4} M) with 1,2-Me_2Hz (2.6×10^{-3} M), measured at 495 nm, pH 9.4, $T = 47$ °C.

The mass balance for the $[Fe(CN)_5X]^{n-}$ ions allows one to conclude that when the concentration of $[Fe(CN)_5NO]^{3-}$ is maximum, all of the initial FeNO has been consumed. In these conditions, the concentration of $[Fe(CN)_5H_2O]^{3-}$ represents around 40% of the initial FeNO, the remainder being $[Fe(CN)_5NO]^{3-}$.

To establish appropriate comparisons with the other hydrazines, we have also carried out experiments at 25 °C for 1,2-Me_2Hz, with variable pH and constant initial concentrations of the reactants. The initial rates of production of $[Fe(CN)_5H_2O]^{3-}$ and $[Fe(CN)_5NO]^{3-}$ are reported in Table 2. Considering the experimental errors, we conclude that the initial rates of formation of both species are similar at constant pH and that both rates have a similar pH-dependence. They show a transition from a proportional dependence to a pH-independent one.

Table 2. Initial Rates of Production, R_{inic} (M/min), of $[Fe(CN)_5H_2O]^{3-}$ and $[Fe(CN)_5NO]^{3-}$ in the Reaction of $[Fe(CN)_5NO]^{2-}$ with 1,2-Me_2Hz, at 25.0 °C

pH	$10^7 \times R_{inic}$ $[Fe(CN)_5H_2O]^{3-}$	$10^7 \times R_{inic}$ $[Fe(CN)_5NO]^{3-}$
8.0	1.85	1.79
9.4	31.3	29.4
10.4	29.0	40.3

Catalysis of Nitrite Reduction by Hz and 1,2-Me_2Hz. In the presence of excess nitrite and Hz, the $[Fe(CN)_5NH_3]^{3-}$ ion catalyzes the reaction described by eq 1. Figure 6 shows the decay of Hz against time for different conditions, and Scheme 1 presents the catalytic cycle. The aquation of $[Fe(CN)_5NH_3]^{3-}$ is fast and practically quantitative.[20,22c] The coordination of NO_2^- into $[Fe(CN)_5H_2O]^{3-}$ is rapidly followed by proton-assisted dehydration (favored by low pH's), leading to bound NO^+. pH's higher than 11 must be avoided because the equilibrium of bound $NO^+-NO_2^-$ species is displaced toward NO_2^-,[8] which is nonreactive toward hydrazine attack. No reaction is detected below pH 7, because of the low concentration of OH^- (see eq 7). We also confirm that Hz is nonreactive toward nitrite in our experimental conditions; that is, in the

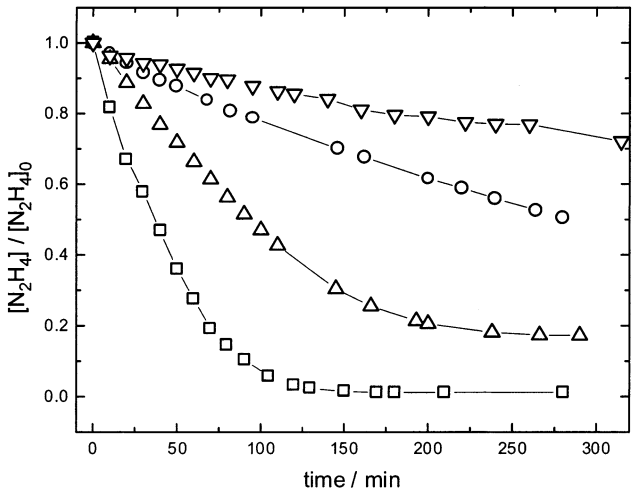

Figure 6. Relative hydrazine decay against time in different reaction conditions, calculated through the yield of produced N_2O established in eq 1. $T = 25.0$ °C; $I = 1$ M, NaCl. $[Hz]_o = 1.3 \times 10^{-2}$ M; $[Fe(CN)_5H_2O^{3-}] = 1.3 \times 10^{-3}$ M. (▽) pH 9.2; $[NO_2^-]$ 0.04 M. (○) pH 7.0; $[NO_2^-]$ 0.12 M. (△) pH 10.2; $[NO_2^-]$ 0.12 M. (□) pH 9.2; $[NO_2^-]$ 0.12 M.

Scheme 1

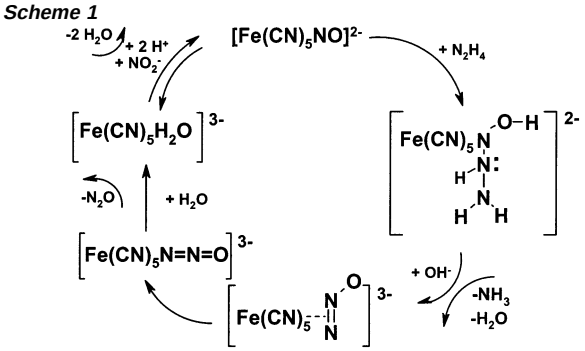

Scheme 2

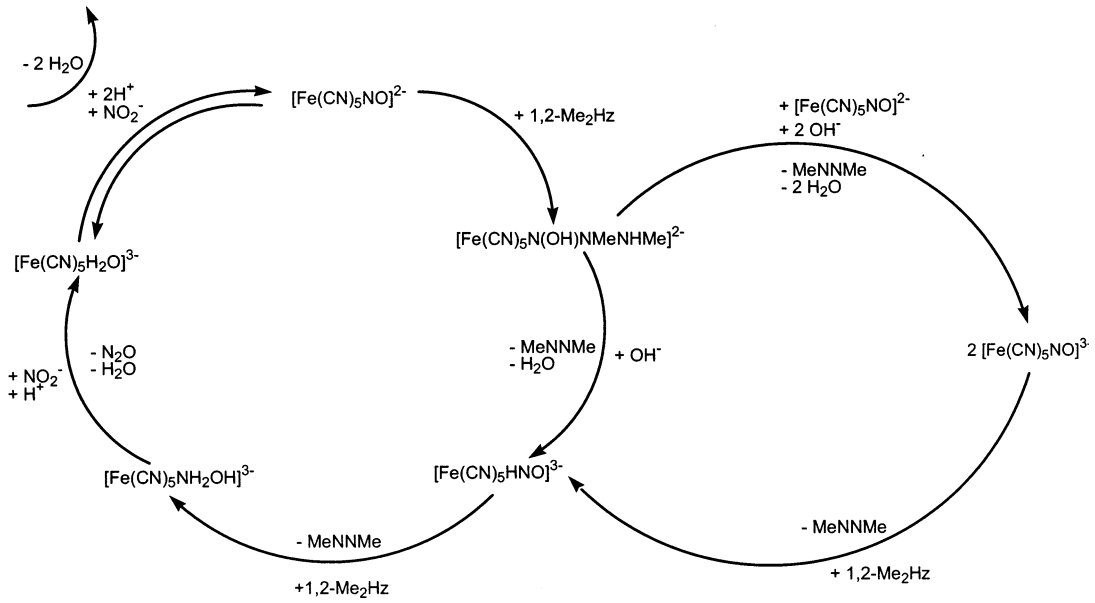

absence of $[Fe(CN)_5NH_3]^{3-}$ or FeNO, no catalytic cycle is observed.

By using 1,2-Me_2Hz as nucleophile, we find that the experiments also show a catalytic cycle, as shown in Scheme 2. However, the reaction products are not the same as those described by eq 5. Although azomethane still appears as the product of 1,2-Me_2Hz oxidation, no NH_3 is found; instead, *N_2O appears as the reduction product of nitrosyl*. Labeling experiments with $^{15}NO_2^-$ show that only $^{15}N_2O$ (molar mass 46) is formed, thus indicating that the reduction product of the cycle involves only the labeled nitrosyl. No catalytic cycle is observed in the absence of $[Fe(CN)_5NH_3]^{3-}$ or FeNO, as shown by the lack of reactivity of 1,2-Me_2Hz toward nitrite in our experimental conditions. The time evolution of the catalytic reaction also shows the initial formation and further decay of the one-electron reduced intermediate, $[Fe(CN)_5NO]^{3-}$.

Discussion

Given the overall stoichiometries described by eqs 1−5 and the pH-dependent reactivities found with the substituted hydrazines, an effort is made to extract some common mechanistic features. We present first an analysis of the reaction mode of Hz, together with the similar reaction modes of MeHz and 1,1-Me_2Hz (i.e., reacting N-atoms close to H but distant to Me). Later, we discuss the alternative process observed with MeHz (reacting N-atom close to Me) and, finally, the distinctive reactivity of 1,2-Me_2Hz.

A. Addition of Hz, MeHz, and 1,1-Me_2Hz. Common Reaction Stoichiometries. We propose that the initial step is a reversible adduct formation comprising the N-atom of the nucleophile and the N-atom of the delocalized {FeNO} moiety (which we identify as $Fe^{15}NO$), as described by eq 6:

$$[Fe(CN)_5{}^{15}NO]^{2-} + NHR_3NR_1R_2 \rightleftarrows [Fe(CN)_5N(OH)NR_3NR_1R_2]^{2-} \quad k_6, k_{-6} \quad (6)$$

This equation has been written in a generalized manner: the R_i substituents are H or Me, depending on the nucleophile under consideration. Although no details of the adduct's structures can be obtained through the kinetic measurements, we assume a deprotonation of the binding N-atom of the nucleophile. The proton could be transferred to the oxygen of the nitrosyl or directly to the medium. These options cannot be distinguished kinetically. We have chosen the first description in eq 6 and further on, on the basis of the fact that the protonated intermediate is actually a stable species, according to our DFT calculations. A second key hypothesis is advanced to explain the reactivity of the different nucleophiles: if another H-atom is bound to the central N (R_3 = H in eq 6), it will be reactive toward OH^-. Further proton transfers and electronic reorganization consummate the reaction. Thus, eq 6 is followed by eq 7:

$$[Fe(CN)_5{}^{15}N(OH)NHNR_1R_2]^{2-} + OH^- \rightarrow [Fe(CN)_5H_2O]^{3-} + N^{15}NO + NHR_1R_2 \quad k_7 \quad (7)$$

Equations 6 and 7 describe the reaction of Hz (R_1 = R_2 = H), giving NH_3 as a product. They can also be used for MeHz in one of its reactive modes, predominant at pH's below 7 (R_1 = H, R_2 = Me), rendering $MeNH_2$ as a product and, finally, for 1,1-Me_2Hz in its main reactive mode (R_1 = R_2 = Me), giving this time Me_2NH as a product. In all of the cases, isotopic labeling is conclusive for the identification of $N^{15}NO$. The absence of labels at the released ammonia and amines also indicates that cleavage of the N−N bond must occur. The fact that MeHz reacts predominantly at low pH's through the addition of the nonsubstituted N-atom is probably related to a preferential protonation at the other N-atom.[34]

It is generally assumed that these electrophilic reactions comprise an initial reversible adduct-formation step.[4,5] Direct crystallographic evidence on the structure of the adduct intermediates only exists for $[Ru(bpy)_2Cl(NO)SO_3]$,[35] but spectrophotometric and kinetic results provide some evidence in the studies with thiolates as nucleophiles.[36] The activation param-

(34) (a) Condon, F. E. *J. Org. Chem.* **1972**, *37*, 3608−3615. (b) Bagno, A.; Menna, E.; Mezzina, E.; Scorrano, G.; Spinelli, D. *J. Phys. Chem. A* **1998**, *102*, 2888−2892.
(35) Bottomley, F.; Brooks, V. F.; Paez, D. E.; White, P. S.; Mukaida, M. *J. Chem. Soc., Dalton Trans. (1972−1999)* **1983**, 2465−1472.
(36) (a) Johnson, M. D.; Wilkins, R. G. *Inorg. Chem.* **1984**, *23*, 231−235. (b) Schwane, J. D.; Ashby, M. T. *J. Am. Chem. Soc.* **2002**, *124*, 6821−6823.

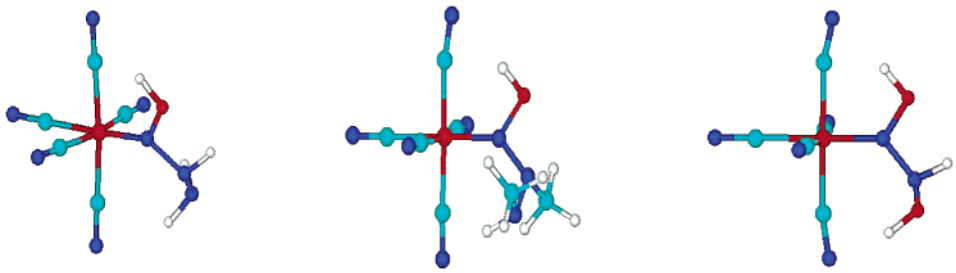

Figure 7. Structures of the adducts formed in the first step of the reaction of $[Fe(CN)_5NO]^{2-}$ with nitrogen hydrides: (a) Hz (eq 6); (b) MeHNNHMe (eq 11); (c) hydroxylamine, NH_2OH.

eters for the reaction with Hz are of similar magnitude and sign as those reported for related additions into FeNO.[8,36] The negative activation entropies are consistent with an associative mechanism. Some spectral evidence on nitrosohydrazine intermediates has been advanced for the reactions of nitrous acid with hydrazines and substituted hydrazines,[37] as well as for the addition reactions of hydroxylamine and azide into FeNO.[38] As our kinetic experiments show no spectral indication of intermediate adduct formation, we carried out a DFT study on reaction 1. We show in Figure 7a the structure of the stable minimum found for the Hz adduct. Similar displays are calculated for MeHz and 1,1-Me_2Hz (not shown). A complete DFT analysis is presented below.

By applying a steady-state treatment to the adduct species in eqs 6 and 7, we derive the following expression for the specific reaction rate, $k_{calc} = k_6/(1 + 10^{(pKo - pH)})$. It has the same form as the experimental rate law, with $pK_o = k_7 \times K_w/k_{-6}$, and K_w having its habitual meaning. The pH-dependence accounts for the role of OH^- in eq 7. It also includes all of the possible influence of hydrazine protonation equilibria, either as the free or as the bound species. In our present study, we discard a direct attack of OH^- on nitrosyl, because this reaction is known to be significantly competitive only above pH 10.[8] Table 1 shows the calculated values for k_6 and k_7/k_{-6}.

The products in eqs 1, 2, and 4 reflect a novel behavior of hydrazine in the reactions with metal or nonmetal oxidants. The usual product of hydrazine oxidation reactions is N_2, with diazene, N_2H_2, being considered a key intermediate which further disproportionates into N_2 and N_2H_4 (or into HN_3 and NH_3).[14] In the present study, the formation of $N_2O + NH_3$ needs adduct reorganization, with successive proton loss at the central N-atom. The strong repulsions of the free electron pairs with the N−N bonding pair result in N−N heterolytic cleavage, along with the central N-atom acting through a combined two-electron transfer to the formally NO^+ ligand, and a one-electron transfer to the terminal N-atom. The cleavage of the N−N bond and the formation of NH_3 by a two-electron oxidant are novel features in the mechanistic redox chemistry of Hz. The generally accepted rule that ammonia production occurs only for one-electron oxidants needs to be modified.[14]

In the reactions of hydrazine with nitrous acid, Stedman proposed that the nitrosation process may evolve through competitive formation and further decomposition of the *cis*- and *trans*-nitrosohydrazines.[37] Each of them could decompose by parallel paths. Under strongly acidic conditions and a high excess of hydrazine, the acid-catalyzed path leading to $HN_3 + H_2O$ was shown to be nearly exclusive. The alternative path leading to $N_2O + NH_3$ was shown to compete at higher pH's. Both paths seem to proceed with complexes $[Ru^{II}(NH_3)_5NO]^{3+}$ [13a] and $[M^{II}(pdma)_2Cl(NO)]^{2+}$ (M = Ru, Os; pdma: *o*-phenylenebis(dimethylarsine)),[13b] where N_2O and N_2 have been also found (although not NH_3). On the other hand, the results with FeNO, strongly supported by the stoichiometry and the ^{15}N labeling experiments, constitute the first report on the rigorously quantitative and *exclusive* appearance of the $N_2O + NH_3$ path. The contrast with the other complexes is a matter of some speculation. Stedman suggested that the fragment attached to NO (MX_5 in our case) could influence the relative rates of formation of the *cis*- or *trans*-nitrosohydrazines. Each of them could give rise to different proportions of NH_3 or HN_3.[37a] Alternatively, the distribution of products could be related to the overall charge of the electrophiles. It is probable that the positively charged complexes facilitate proton loss from the terminal nitrogen and water removal, leading to bound azide. In contrast, negatively charged FeNO favor the retention of protons and NH_3 release after the heterolytic cleavage of the N−N bond.

B. Alternative Reaction Paths for MeHz and 1,1-Me_2Hz. Intermediate Dimer Formation. A pH higher than 8 favors a new reaction path for MeHz, whose stoichiometry is described by eq 3. In eq 6, the adduct contains R_3 = Me and $R_1 = R_2$ = H. Note that at this pH both N-atoms of MeHz are deprotonated and that the methylated-N is probably more nucleophilic.[34] The adduct intermediate has no reactive H at the central N-atom; OH^- may then react as in eq 8:

$$[Fe(CN)_5{}^{15}N(OH)NMeNH_2]^{2-} + OH^- \rightarrow [Fe(CN)_5{}^{15}N(OH)NMeNH]^{3-} + H_2O \quad k_8 \quad (8)$$

The product of eq 8 is probably responsible of the persistent absorbance at 480 nm. This could be traced to a MLCT transition to the N=N chromophore, as suggested by our TD-DFT calculations.[33] The deprotonated adduct may react as a nucleophile toward another FeNO, giving the dimer $[Fe(CN)_5{}^{15}N(OH)NMeN{}^{15}N(OH)Fe(CN)_5]^{5-}$, which, induced by OH^- attack, may further rearrange by cleavage at the unlabeled N−N bond and displacement of the Me group, eq 9:

(37) (a) Perrott, J. R.; Stedman, G.; Uysal, N. *J. Chem. Soc., Dalton Trans. (1972−1999)* **1976**, 2058−2064. (b) Perrott, J. R.; Stedman, G.; Uysal, N. *J. Chem. Soc., Perkin Trans. 2* **1977**, 274−278.
(38) Wolfe, S. K.; Andrade, C.; Swinehart, J. H. *Inorg. Chem.* **1974**, *13*, 2567−2572.

$$[Fe(CN)_5{}^{15}N(OH)NMeN^{15}N(OH)Fe(CN)_5]^{5-} + OH^- + H_2O \rightarrow 2[Fe(CN)_5H_2O]^{3-} + {}^{14}N^{15}NO + N^{15}N + MeOH \quad (9)$$

We remark that *both* types of nucleophilic attack (i.e., from the methylated and nonmethylated N-atoms) occur at pH higher than 8 and that this is supported by the stoichiometries of reactions 2 and 3 and by the yields of gaseous products. The formation of the dimer and subsequent reaction according to eq 9 are consistent with the labeling experiment, indicating that cleavage at the unlabeled N−N bond must occur.[39] Stedman also found similar results and proposed a related explanation for the nitrosation of MeHz when reacting with nitrous acid.[37b] A possible decomposition of the dimer in two steps could be also proposed, with release of N_2O followed by transient stabilization of the mononuclear species, $[Fe(CN)_5N(OH)NMe]^{3-}$. The latter would decompose giving N_2 and MeOH.[37b]

A critical situation is presented when considering 1,1-Me_2Hz, as adduct formation should involve the N-atom bound to both Me groups. In fact, 1,1-Me_2Hz shows a negligible contribution from this path to the rate, suggested by the weak shoulder found at 480 nm when the degree of conversion for the main reaction (eq 4) has attained a maximum value. The picture seems to be similar to the one described for MeHz in eqs 8 and 9, but the corresponding species is found to be nonreactive, as no decomposition path affording products is observed.

By applying a steady-state treatment to the concentration of both types of adducts, in eqs 6−8, we obtain:

$$k_{calc} = k_{6a}/(1 + 10^{[pK_1 - pH]}) + k_{6b}/(1 + 10^{[pK2 - pH]}) \quad (10)$$

where k_{6a} and k_{6b} represent the specific rate constants for the formation of adducts with R_3 = H or Me, respectively; $pK_1 = k_7 \times K_w/k_{-6a}$, $pK_2 = k_8 \times K_w/k_{-6b}$. For the reactions of Hz and 1,1-Me_2Hz, $k_{6b} = 0$, and, for MeHz, both terms are considered. Figure 4 includes the results of the nonlinear fitting process to eq 10, and the resultant kinetic parameters are displayed in Table 1.

In the previous considerations, we discarded that the production of N_2 and MeOH could result from the reaction of $MeNH_2$ (generated in the main path, eq 2) with FeNO. The reactions of primary amines with FeNO have been studied[40a] and are very slow as compared with the observed path in our system (eq 3). However, catalysis of the addition reactions of amines has been proposed.[40b]

(39) Additional evidence of the mechanism proposed in eqs 8 and 9 is provided by some complementary observations during the gas production experiments. When dealing with more concentrated solutions of reactants (see Experimental Section), we found that the increase in the concentration of MeHz (at constant FeNO) was accompanied by an increase and further sharp decrease of gas production. We interpret this result through the formation of more adducts at higher MeHz concentrations (eq 6). The *N*-methylated binding adduct is more stable than the one implying binding through the nonmethylated N, as k_{6b} is higher than k_{6a}, and k_{-6} is supposed to be the same for both adducts, see eq 10. While one adduct leads to $N_2O + MeNH_2$ upon decomposition, the other one needs another FeNO for dimer formation. Thus, free FeNO is consumed after an initial period of normal behavior. The rate decreases, with slow evolution of N_2, N_2O, and MeOH, along with the ability of the methylated adduct to release FeNO. A similar behavior is observed when the concentration of FeNO is reduced, at constant MeHz concentration. This interpretation is consistent with the production of N_2 (molar mass 29) and the persistence of the 480 nm shoulder when the production of the aqua-ion has finished.

(40) (a) Dozsa, L.; Kormos, V.; Beck, M. T. *Inorg. Chim. Acta* **1984**, *82*, 69−74. (b) Kathó, A.; Beck, M. T. *Inorg. Chim. Acta* **1988**, *174*, 99−102.

C. Reaction of FeNO with 1,2-Me_2Hz. A Different Mechanism. The reactivity pattern of 1,2-Me_2Hz is different from the others. $^{15}NH_3$ is produced (not N_2O) through a six-electron reduction process of bound-$^{15}NO^+$. Two-electron oxidation of the nucleophile leads to azomethane, a behavior consistent with eq 5. We propose eqs 11−17 to describe the associated mechanism. Equation 11 represents an initial adduct formation, similar to others (see Figure 7b, which shows that addition is not sterically hindered), and in agreement with the general eq 6 (previously formulated, with R_1, R_3 = Me; R_2 = H). Reaction 11 is followed by a two-electron transfer from 1,2-Me_2Hz to the bound N-atom (eq 12).

$$[Fe(CN)_5{}^{15}NO]^{2-} + MeHNNHMe \rightleftarrows [Fe(CN)_5{}^{15}N(OH)NMeNHMe]^{2-} \quad k_{11}, k_{-11} \quad (11)$$

$$[Fe(CN)_5{}^{15}N(OH)NMeNHMe]^{2-} + OH^- \rightarrow [Fe(CN)_5H^{15}NO]^{3-} + MeNNMe + H_2O \quad k_{12} \quad (12)$$

Equation 12 has some resemblance to eq 7, in the sense that N(+1) products are formed. However, in reaction 7, N_2O did not require the previous formation of intermediate NO/HNO species. Our inference that two H atoms vicinal to the binding N should be present for promoting the discussed mechanism (i.e., the cleavage of the N−N bond) can be relaxed now, because 1,2-Me_2Hz is able to transfer two electrons and two protons to form a very stable product, azomethane. Thus, the bound nitroxyl species, HNO, can be formed (eq 12) and survive long enough to react with another 1,2-Me_2Hz, avoiding N_2O formation.

Although we cannot show spectral evidence for HNO, its intermediate character appears as the only way to explain the stoichiometry and labeling results. Spectroscopic and structural evidence[41] show that HNO is an identifiable ligand in related low-spin d^6 ruthenium and osmium complexes, and DFT calculations also predict its existence in two-electron-reduced FeNO.[42]

In eqs 13 and 14, we propose additional two-electron transfers to form $[Fe(CN)_5{}^{15}NH_2OH]^{3-}$ and $[Fe(CN)_5{}^{15}NH_3]^{3-}$, respectively:

$$[Fe(CN)_5H^{15}NO]^{3-} + MeHNNHMe \rightarrow [Fe(CN)_5{}^{15}NH_2OH]^{3-} + MeNNMe \quad k_{13} \quad (13)$$

$$[Fe(CN)_5{}^{15}NH_2OH]^{3-} + MeHNNHMe \rightarrow [Fe(CN)_5{}^{15}NH_3]^{3-} + MeNNMe + H_2O \quad k_{14} \quad (14)$$

The first product is a well-characterized species,[43] which is also obtained in the irreversible electrochemical reduction of FeNO.[44] A full six-electron conversion of NO^+ to NH_3 was

(41) (a) Wilson, R. D.; Ibers, J. A. *Inorg. Chem.* **1979**, *18*, 336−343. (b) Southern, J. S.; Hillhouse, G. L. *J. Am. Chem. Soc.* **1997**, *119*, 12406−12407. (c) Lin, R.; Farmer, P. J. *J. Am. Chem. Soc.* **2000**, *122*, 2393−2394. (d) Sellmann, D.; Gottschalk-Gaudig, T.; Hausinger, D.; Heinemann, F. W.; Hess, B. A. *Chem.-Eur. J.* **2001**, *7*, 2099−2103.

(42) González Lebrero, M. C.; Scherlis, D. A.; Estiú, G. L.; Olabe, J. A.; Estrin, D. A. *Inorg. Chem.* **2001**, *40*, 4127−4133.

(43) The $[Fe(CN)_5NH_2OH]^{3-}$ ion has been spectroscopically and kinetically characterized by us through its formation reaction, starting from $[Fe(CN)_5H_2O]^{3-}$ ion and NH_2OH, in equimolar conditions (unpublished observations).

(44) Masek, J.; Maslova, E. *Collect. Czech. Chem. Commun.* **1974**, *39*, 2141−2160.

found with $[Ru(NH_3)_5NO]^{3+}$, using Cr(II),[15] as well as in the electrocatalytic reduction of iron nitrosyl-porphyrines,[16] where Fe−HNO and $Fe-NH_2OH$ intermediates have also been proposed.

The results show that another parallel path is operative for describing the stoichiometry in eq 5. We propose eqs 15−17 for the formation and slow decay of the one-electron reduced species, $[Fe(CN)_5NO]^{3-}$.

$$[Fe(CN)_5{}^{15}N(OH)NMeNHMe]^{2-} + [Fe(CN)_5{}^{15}NO]^{2-} + 2OH^- \rightarrow 2[Fe(CN)_5{}^{15}NO]^{3-} + MeNNMe + 2H_2O \quad k_{15} \quad (15)$$

$$[Fe(CN)_5{}^{15}NO]^{3-} + MeHNNHMe \rightarrow [Fe(CN)_5{}^{15}N(OH)NMeNHMe]^{3-} \quad k_{16} \quad (16)$$

$$[Fe(CN)_5{}^{15}N(OH)NMeNHMe]^{3-} + [Fe(CN)_5{}^{15}NO]^{3-} \rightarrow 2[Fe(CN)_5{}^{15}HNO]^{3-} + MeNNMe \quad k_{17} \quad (17)$$

This proposal is based on the assumption that 1,2-Me_2Hz *always* behaves as a two-electron donor, sustaining the stoichiometry experimentally found (eq 5). Thus, *two* $[Fe(CN)_5{}^{15}NO]^{3-}$ ions must react with 1 mol of nucleophile to obtain the two-electron reduced product, $[Fe(CN)_5{}^{15}HNO]^3$ (eq 17). The latter reacts subsequently as in reactions 13 and 14. Remarkably, the maximum concentration of $[Fe(CN)_5{}^{15}NO]^{3-}$ is obtained when nearly all of the initial FeNO has been transformed. The results shown in Figures 3 and 4 indicate that reactions 11−14 (the two-electron path) and 15 (the one-electron path) evolve with similar rates. Accumulation of the radical species is traced to the weaker electrophilic character of $[Fe(CN)_5NO]^{3-}$ as compared to FeNO. Certainly, the reduction of $[Fe(CN)_5NO]^{3-}$ also occurs at a more negative potential than the one required to reduce FeNO.[44]

The existence of one-electron and two-electron paths for the same nucleophile is an interesting feature. Although 1,2-Me_2Hz appears as requiring a two-electron process for the generation of a stable oxidation product, it can meet the alternative requirements found for nitrosyl, attaining one- or two-electron reduction through the reaction with one or two mononuclear FeNO moieties, respectively.

Given that the current experimental evidence on nitrosyl reduction processes shows that the occurrence of two-electron, four-electron, or six-electron reduction products depends on the metal-coligand environment, the reductant, and the pH conditions,[15,16] the present study sheds light on the nature of the different, kinetically controlled processes associated with the structures of the nucleophile reductants for a common electrophile.

D. Rate Comparisons for the Addition Reactions of Different Hydrazines to FeNO. As a result of the mechanistic analysis, Table 1 displays the rate-constant values obtained for the different nucleophiles. It can be seen that the main changes in the rates correspond to the elementary steps comprising adduct formation. For the three nucleophiles attacking through the NH_2 groups (k_{6a} values in eq 6), the rates decrease with increased methylation by about a factor of 10 for each Me-substitution. Similar, although unexplained, trends were found in the reactions of Hz and substituted hydrazines with nitrous acid.[37b] In fact, it is difficult to ascribe these changes to the predominant influence of any of the potential factors, the basicity, the nucleophilicity, solvational effects, or steric restrictions afforded by methylation. For MeHz, the rate for the adduct formation occurring through the methyl-substituted N (k_{6b}) is significantly higher than k_{6a}, suggesting a greater nucleophilicity, in agreement with recent NMR and quantum chemical calculations.[34] Finally, the adduct-formation rate for 1,2-Me_2Hz (k_{11}) is the lowest. The quotients of the specific rates of adduct decomposition were found to be practically constant, although the values for the N-substituted paths are lower by around an order of magnitude (consistent with the observed slow rates). If we assume that the mechanisms of these reactions are similar to that proposed for OH^- additions, and that the values of k_{-6} (or k_{-11}) are all similar (ca. 0.07 s^{-1}),[8b] we calculate values of around 10^5-10^4 M^{-1} s^{-1} for k_7 (or k_8, k_{12}). These rate constants are quite consistent with bond reorganization processes initiated by proton transfer from a weak acid to external OH^-.[45] Finally, the value of k_6 for Hz is consistently comparable with the values measured for the addition processes with related N-binding nucleophiles, azide and hydroxylamine.[38]

E. Catalysis of Nitrite Reduction by Pentacyano(aqua)-ferrate(II). An important feature of the nitrosation reactions is that the $[Fe(CN)_5]^{3-}$ moiety is conserved along the reaction (cf. eqs 1−5). The $[Fe(CN)_5H_2O]^{3-}$ ion (which is generated in situ by starting from FeNO or $[Fe(CN)_5NH_3]^{3-}$) contains the active site able to bind to a diversity of ligands L present in the medium. Coordination of nitrite, fast conversion to NO^+, further attack by hydrazine, and fast N_2O release lead to regeneration of $[Fe(CN)_5H_2O]^{3-}$. Other potential ligands (L = NH_3, N_2H_4) may compete for the active site, but catalysis proceeds in appropriate pH conditions (see Results) if sufficient nitrite is in excess. In Scheme 1, we include the linkage isomers of N_2O, as shown later by the DFT calculations.

An interesting deviation from the above-discussed process is shown by the reaction of FeNO with 1,2-Me_2Hz (eq 5), which also operates catalytically in the presence of nitrite and reductant. Now the product reveals the formation of azomethane and N_2O, in contrast with the six-electron full reduction to NH_3 occurring in eq 5. Scheme 2 displays the proposed cycle, which also contains the contribution of the $[Fe(CN)_5NO]^{3-}$ path (right side). As we find no reason for different reduction paths in the catalytic and stoichiometric experiments, we believe that nitrite traps the NH_2OH intermediate in eq 13, promoting a comproportionation, coupling reaction giving N_2O. This is supported by the experiments with $^{15}NO_2^-$ leading *only* to $^{15}N_2O$. The reaction of FeNO with hydroxylamine is known to generate $N_2O + H_2O$, through an addition mechanism similar to the one described in the present work.[38] In contrast, if no excess nitrite is present, the bound N(+1) and N(−1) intermediates formed in eqs 12 and 13 can survive sufficiently for being rapidly attacked by the excess reductant.

F. Comparisons with Nitrite Reductase Enzymes. The catalysis of nitrite reduction by $[Fe(CN)_5H_2O]^{3-}$ has some resemblance with the behavior of the dissimilatory nitrite reductases.[10] These enzymes catalyze the *one-electron* reduction of bound NO^+, promoted by an intramolecular electron transfer

(45) Ruff, F.; Csizmadia, I. G. *Organic Reactions Equilibria, Kinetics, and Mechanism*; Elsevier: New York, 1994.

followed by fast release of NO.[46] The enzymes also catalyze the nitrosation reactions of nitrogen hydrides (N_2H_4, NH_2OH, HN_3), probably through a much less efficient competitive path.[47] It appears that the initial coordination of nitrite and its conversion to NO^+ are similar for nitrite reductases and $[Fe(CN)_5H_2O]^{3-}$. However, with $[Fe(CN)_5H_2O]^{3-}$, the redox process is entirely localized at the nitrosyl-Hz adduct, and no redox Fe(II)−Fe(III) cycles are operative. From the comparison of both systems, we conclude that the common NO_2^- $-NO^+$ initial step is followed, for the pentacyanoferrates, by the reduction of nitrite to N_2O, rather than to NO. At this point, it is interesting to remark that some fungal nitric oxide reductases are capable of achieving quantitative conversion of NO_3^- and NO_2^- to N_2O (fungal denitrification), a process likely to be important in forest soils.[10] Connections to our present system are evident if we consider that these fungi are capable of catalyzing a process termed "codenitrification", in which $^{15}NO_2^-$ is reduced to $(^{14}N,^{15}N)_2O$ in the presence of $^{14}NH_4^+$ or $^{14}N_3^-$.[48] Finally, our results demonstrate that the formation of the N−N bond of N_2O in the process of nitrosyl reduction is efficiently achieved by the attack of nucleophiles. In contrast, the generation of N_2O by dimerization of nitroxyl species (either bound or dissociated) is not favored. The bound Fe−HNO ligand appears to be sufficiently long-lived to be quantitatively reduced to hydroxylamine and NH_3, provided appropriate conditions stand (e.g., with 1,2-Me_2Hz as a reductant).

G. DFT Calculations on the Adduct Formation and Subsequent Reactions of FeNO with Hydrazine. Formation and Interconversion of η^2- and η^1-N_2O Linkage Isomers. The reaction profile has been analyzed for the different steps of eq 1. Geometry optimization shows that several true minima can be found in the potential hypersurface, in addition to those related to reactants and products. In addition to the Hz adducts previously described, and shown in Figure 7a,b, we have calculated a similar structure for the adduct formed by hydroxylamine addition (Figure 7c), suggesting a common pattern with other nitrogen hydrides as well.[38] Table 3 summarizes the relevant calculated distances, angles, and IR wavenumbers. By comparing with FeNO, it can be seen that the essentially linear FeNO moiety transforms into a bent structure upon adduct formation. The Fe−N−O and Fe−N−N angles are around 122° and 133°, respectively, and the Fe−N and N−O distances are significantly elongated as compared to the ones in FeNO (1.615 and 1.16 Å, respectively). The N−O distance is consistent with a double-bond character, as estimated for $[Fe(CN)_5HNO]^{3-}$.[42] The $N-N_1$ and $N_1-N_2(O)$ distances agree with those found in hydrazine unidentate complexes.[49] Computed values for the relevant IR frequencies agree with expectations: the values of $\nu_{NOH(N)}$ and $\nu_{NNH(N)}$ are in the region of stretching and rocking vibrations found for hydrazine complexes,[21,50] and the ν_{CN} values are as expected for Fe(II) pentacyano complexes containing π-acceptor L ligands.[50]

For both cases, deprotonation of the adducts also renders stable intermediates. The protonated species are about 1.5 eV less stable than the deprotonated ones. Intense charge-transfer (CT) bands are calculated for the latter around 410 nm, associated with metal-to-ligand transitions centered in the NO moieties.

Table 3. Calculated Distances (Å), Angles (deg), and Selected IR Data (cm^{-1}) for $[Fe(CN)_5NO]^{2-}$ (FeNO), and Intermediates Formed in the Reactions with Hz and 1,2-Me_2Hz (Included Are the N_2O Complexes)

	FeNO	Hz	1,2-Me_2Hz	η^2-N_2O[a,b]	η^1-N_2O[a,b]
Fe−N	1.615	1.785	1.796	2.075, 1.992	1.820
N−O	1.160	1.376	1.378	1.254	1.242
$N-N_1$[c]		1.365	1.405	1.191	1.138
N_1-N_2[d]		1.405	1.402		
Fe−C cis	1.959	1.962	1.962	1.975	1.990
trans	1.965	1.972	1.957	1.949	1.962
C−N cis	1.169	1.172	1.172	1.175	1.176
trans	1.168	1.172	1.170	1.175	1.176
∠FeNO	179.9	123.0	121.3	142.5	-
$\angle FeNN_1$		133.0	134.5	76.8	179.8
$\angle NN_1N_2$		115.8	116.7		
$\angle N_1NO$				140.6	178.8
$\nu_{NOH(N)}$		1008	1009		
		1490; 1311	1469		
$\nu_{NNH(N)}$		1060	1054		
ν_{N_1NO}				1159; 659	2287; 1120
ν_{N_1N}				1812	
ν_{CN}	2160−2170	2127−2172	2136−2174	2127−2147	2115−2131

[a] Distances in free N_2O: N−N, 1.128 Å; N−O, 1.184 Å (ref 9). [b] Fundamental IR wavenumbers in free N_2O: ν_1 (asymmetric stretch), 1285 cm^{-1}; ν_2 (bending), 589 cm^{-1}; ν_3 (symmetric stretch), 2224 cm^{-1} (ref 9). [c] N_1: N-atom bonded to nitrosyl. [d] N_2: N-atom bonded to N_1.

The linear-to-bent transformations in the {MNO} moieties have been associated with electronic redistributions involving changes in coordination number of the metals.[51] Bending has also been found upon reduction of the nitrosyl ligand in a given coordination environment.[41,42] The two-electron transfer to the delocalized FeNO moiety involves a change in coordination at the nitrosyl N-atom, which can be formally described by means of a hybridization change from sp to sp^2. The intermediate's FeNO angle, 123°, is similar to the one found in the conversion of bound NO^+ to HNO.[41,42]

The DFT calculations show another energy minimum along the reaction coordinate, whose geometry is displayed in Figure 8. It corresponds to the product of adduct decomposition, still containing bound N_2O. To our surprise, the N_2O ligand shows an *unprecedented* η^2 side-bound coordination mode. The structure associated with this coordination mode results from a geometry minimization starting from the first adduct of Figure 8, after subtraction of NH_3, that is, from an angular N_2O complex coordinated by the central N-atom. No structural information exists on N_2O complexes,[9] even for the reasonably pure salts of the $[Ru(NH_3)_5N_2O]^{2+}$ ion,[52a] where N_2O is assumed to bind in a η^1 linear mode through the terminal N-atom.[52b,c] The η^1 linear mode, also shown in Figure 8, is also a minimum in the potential hypersurface, according to our calculations. The reaction scheme, shown in the same figure, justifies the existence of both minima in the reaction coordinate. Linear η^1 coordination is not easily attained in a single step from the initial adduct, as it is the η^2 one that only needs angular reorganization after NH_3

(46) Silvestrini, M. C.; Tordi, M. G.; Musci, G.; Brunori, M. *J. Biol. Chem.* **1990**, *265*, 11783−11787.
(47) Kim, C. H.; Hollocher, T. C. *J. Biol. Chem.* **1984**, *259*, 2092−2099.
(48) Tanimoto, T.; Hatano, K. H.; Kim, D. H.; Uchiyama, H.; Shoun, H. *FEMS Microbiol. Lett.* **1992**, *93*, 177−180.
(49) (a) Heaton, B. T.; Jacob, C.; Page, P. *Coord. Chem. Rev.* **1996**, *154*, 193−229. (b) Bottomley, F. *Quart. Rev.* **1970**, 617−638.
(50) Nakamoto, K. *Infrared and Raman Spectra of Inorganic and Coordination Compounds*, 4th ed.; Wiley: New York, 1986.
(51) (a) Enemark, J. H.; Feltham, R. D. *Proc. Natl. Acad. Sci. U.S.A.* **1972**, *69*, 3534−3536. (b) Song, J.; Hall, M. B. *J. Am. Chem. Soc.* **1993**, *115*, 327−336.
(52) (a) Bottomley, F. *Inorg. Synth.* **1976**, *16*, 75−85. (b) Bottomley, F.; Brooks, W. V. F. *Inorg. Chem.* **1977**, *16*, 501−502. (c) Tuan, D. F.; Hoffmann, R. *Inorg. Chem.* **1985**, *24*, 871−876.

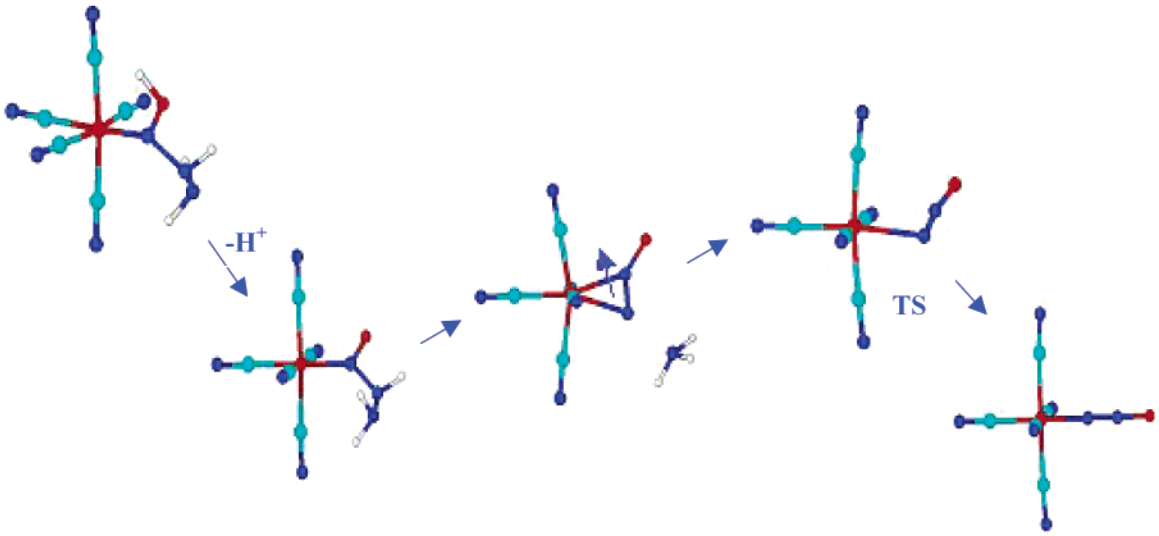

Figure 8. Schematic representation of the calculated stable intermediates formed in initial steps involved in the reaction of $[Fe(CN)_5NO]^{2-}$ with Hz, rendering the N_2O-bound species. The structures correspond to singular points in the potential hypersurface, calculated at a b3lyp-6-31G** level. Relative energies (*y*-coordinate) are not drawn to scale. Arrows indicate changes in the molecule that lead to the next step. All of the adducts and intermediates, except for the first one, bear the charge 3−.

release. Figure 8 also shows the transition-state (TS) structure calculated for the conversion of η^2-N_2O into η^1-N_2O. The calculations show that the TS stands 0.30 eV higher in energy than the η^2 state. The more stable η^1 species lies 0.80 eV lower than the η^2 isomer.

The predicted η^2, side-bound N_2O is a remarkable result, which must be considered in the context of the modern developments on the structure of the photogenerated linkage isomers of small ligands.[53] The results on the MS1 and MS2 states for nitrosyl coordination (end-on, O-bound "isonitrosyl" ligand and η^2, side-bound, respectively)[53] have been recently expanded by the discovery of η^2, side-bound N_2, obtained upon irradiation of the $[Os(NH_3)_5(\eta^1\text{-}N_2)][PF_6]_2$ complex.[54] Table 3 displays the calculated distances, angles, and IR wavenumbers for both N_2O-linkage isomers, which can be compared with values for FeNO and $[Ru(NH_3)_5(\eta^1\text{-}N_2O)]^{2+}$. It can be seen that the Fe−N distance increases in the sense FeNO < η^1 < η^2, reflecting a decrease in bond order (only a σ-bond is postulated for the η^1-mode).[51b,c] The calculated N−N and N−O distances in η^1-N_2O are slightly longer than those in free N_2O, but the difference is greater, ca. 0.06 Å, for η^2-N_2O. This seems reasonable on the basis of predictable $\sigma-\pi$ interactions weakening the two bonds. Interestingly, the FeNN angle of 69.19° is similar to the one found for FeNO in the MS2 state, 65.1°. As in the latter MS2, Figure 8 shows that the equatorial ligands are repelled by the side-on N_2O group. The IR results also show significant shifts in the relevant wavenumbers, which are consistent with the described geometry changes. Thus, η^1-N_2O shows the stretchings associated with the NNO fragment at 2287 and 1120 cm^{-1}, close to those observed for $[Ru(NH_3)_5NNO]^{2+}$.[13b] In contrast, η^2-N_2O shows the absorptions at 1159 and 1812 cm^{-1}. The latter one, strongly downshifted with respect to the one in the η^1 isomer, probably reflects the strong $\sigma-\pi$ interactions of iron with the side-on N═N moiety. The cyanide stretching values can be interpreted in terms of the competing π-acid abilities of cyanide versus those of the N_2O ligands.

In relation to the UV−vis spectra, calculated MLCT bands appear at 323 nm for the η^2-N_2O intermediate (with a shoulder at 451 nm) and at 265 nm for the η^1-N_2O one. They correspond, in both cases, to transitions from an orbital centered in the metal, to the LUMO, delocalized in the N_2O ligand. The 265 nm band is consistent with the one found at 233 nm for the linear $[Ru(NH_3)_5N_2O]^{2+}$ ion.[13a]

Conclusions

The experimental and theoretical results on the electrophilic reactions of FeNO with hydrazine and substituted derivatives as nucleophiles show that a common framework can be proposed for the initial step of the reactions. Reversible adduct formation occurs on the N-atom of the FeNO moiety, with attack of the N-atoms of the nucleophiles and deprotonation. Further redox processes lead to adduct decomposition. The stoichiometries and mechanisms of *both* the oxidation and the reduction processes depend on the nucleophile, with the following important observations: (a) All adduct formations need a first deprotonation of the binding N-atom of the nucleophile to attain reasonable rates. Thus, 1,1-Me_2Hz shows negligible reactivity when the attacking N-atom is bonded to two methyl groups. (b) If a second proton is available at the same position, its loss will be promoted by OH^- attack, leading to N−N bond cleavage, N_2O evolution, and formation of the corresponding amine. This is a two-electron reduction path for nitrosyl, with no formation of intermediates. (c) If the second proton is not available (alternative route for MeHz), N−N bond cleavage is precluded, and a second adduct-formation path with another FeNO leads to N_2 and N_2O, with MeOH release. This path is favored at pH's greater than 8. (d) 1,2-Me_2Hz shows an entirely different behavior. No second proton is available for promoting N−N bond cleavage. Instead, electron and proton loss lead to azomethane, coupled with three successive, two-electron-transfer reductions from NO^+ down to NH_3, with HNO- and NH_2OH-

(53) (a) Coppens, P.; Novozhilova, I.; Kovalevsky, A. *Chem. Rev.* **2002**, *102*, 861−884. (b) Carducci, M. D.; Pressprich, M. R.; Coppens, P. *J. Am. Chem. Soc.* **1997**, *119*, 2669−2678.
(54) Fomitchev, D. V.; Bagley, K. A.; Coppens, P. *J. Am. Chem. Soc.* **2000**, *122*, 532−533.

bound intermediates. The above reaction also shows a parallel path with an initial rate similar to the one previously discussed. It occurs through one-electron transfer to FeNO, showing a fast formation and slow decay of the NO-radical species. The mechanism needs two FeNO molecules to satisfy the two-electron reducing ability of 1,2-Me_2Hz. (e) For the reaction with hydrazine, the $[Fe(CN)_5H_2O]^{3-}$ ion is a product which may bind nitrite (as NO^+) and be further attacked by the nucleophile, promoting a two-electron catalytic reduction of nitrite to N_2O, with concomitant production of NH_3. (f) 1,2-Me_2Hz also promotes the catalytic reduction of nitrite to N_2O, although a different mechanism is involved, with azomethane as the oxidation product.

The theoretical DFT calculations of the potential hypersurfaces show true minima for adduct formation in the different cases, as well as for the Fe−N_2O bound intermediates formed afterward. Most significant are the detection of side-bound, η^2-N_2O, as well as its evolution to the more stable η^1-linkage isomer. The elucidation of the mechanistic features of this complete set of reactions is relevant to denitrification processes occurring in different natural media and has evident connections with the role of the enzymes participating in nitrosyl−nitrite reduction reactions. It is likely that related adduct formation and decomposition paths are operative for the reactions of other nitrogen hydrides (NH_3, NH_2OH, N_3^-) with nitroprusside.

Acknowledgment. This work was supported by the Universities of Buenos Aires, Mar del Plata and La Plata, the Argentinian agencies Anpcyt and Conicet, and by the VolkswagenStiftung. V.T.A., G.L.E., and J.A.O. are members of the scientific staff of Conicet.

Supporting Information Available: Figures SI 1 (successive spectra for the reaction of FeNO with 1,1-Me_2Hz), 2 (EPR spectrum of $[Fe(CN)_5NO]^{3-}$), 3−5 (first-order and second-order plots for the reactions with Hz, MeHz, and 1,1-Me_2Hz, respectively), 6 (Eyring plot for the reaction with Hz) (PDF). This material is available free of charge via the Internet at http://pubs.acs.org.

JA025995V